Journal of Computer-Aided Molecular Design, 1 (1987) 97–120
ESCOM
J-CAMD 010

Strategic approaches to drug design. II. Modelling studies on phosphodiesterase substrates and inhibitors

A. Davis, B.H. Warrington and J.G. Vinter

Smith Kline & French Research, The Frythe, Welwyn, Herts AL6 9AR, U.K.

Received 20 April 1987
Revised 9 May 1987
Accepted 15 May 1987

Key words: Phosphodiesterase inhibitors; Cyclic nucleotides; Molecular modelling

SUMMARY

Modelling studies have been carried out on the phosphodiesterase (PDE) substrates, adenosine- and guanosine-3′5′-cyclic monophosphates, and on a number of non-specific and type III-specific phosphodiesterase inhibitors. These studies have assisted the understanding of PDE substrate differentiation and the design of potent, selective PDE type III inhibitors.

INTRODUCTION

Phosphodiesterase (PDE) enzymes, which hydrolyse adenosine- and guanosine-3′5′-cyclic monophosphates (cAMP, cGMP, see Fig. 1) to the corresponding 5′-monophosphates, differ with species and tissue type. In any tissue there may be several distinguishable PDE isozymes with differing selectivity for cAMP and cGMP, activators and catalytic requirements [1]. The variability of enzymes, isozymes or preparations used by different workers has made structure-activity studies of PDE enzyme inhibitors extremely difficult. We report here the results of modelling studies on the natural substrates (cAMP and cGMP), non-specific PDE inhibitors (compounds which have been shown to inhibit the activity of more than one PDE isozyme) and specific PDE type III inhibitors.

METHODS

Modelling was performed using the COSMIC and ASTRAL [2] software frameworks developed in-house and running on Microcolour M2250, Sigmex 6110 and Evans & Sutherland PS330 terminals from a Digital Equipment VAX 11/780. Phosphodiesterase isoenzymes were isolated and assayed as described by Reeves et al. [3]. IC_{50} values were obtained by incubation of PDE III (the low K_m, Ca-calmodulin insensitive isozyme) from cat ventricle at 1μM cAMP and a wide

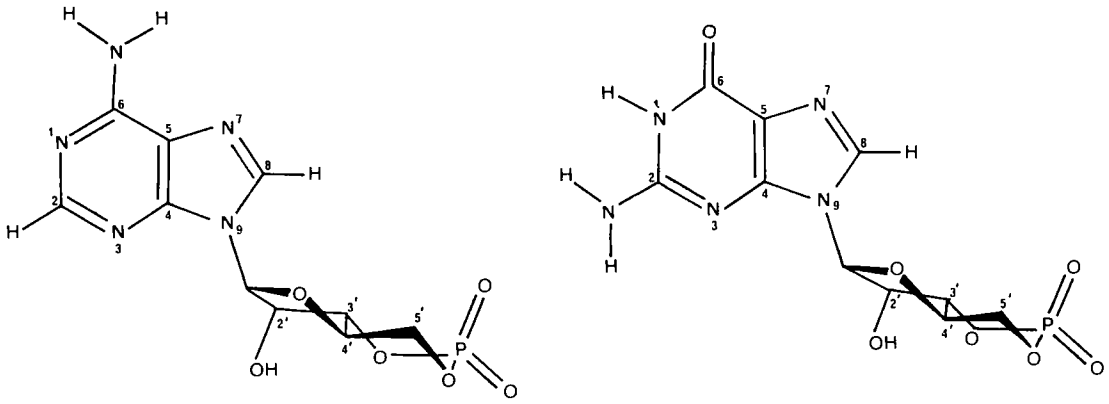

Fig. 1. Adenosine (left) and Guanosine (right) -3'5'- cyclic monophosphates.

range of inhibitor concentrations. Data were analysed by a non-linear least squares logistic fit program. Selectivity for PDE III was confirmed by similar determinations using other single PDE isoenzymes.

STUDIES ON cAMP AND cGMP

Conformational Preferences

Any analysis of enzymic recognition of cyclic nucleotides is critically dependent on the active conformation used for modelling, since distances between possible binding groups are affected by rotation of the purine and by flexing of the ribose-3'5'-cyclic phosphate (RcP) ring system.

The Cambridge Crystallographic Database was searched for the RcP system. The search yielded a total of eight compatible structures with coordinate data, based on derivatives of cAMP, cGMP, cCMP and cIMP.

Examination of the retrieved structures showed that all had very similar conformations in the RcP system (Figs. 2 and 3). The structures differed markedly, however, in the torsional angle about the riboside (purine-ribose) bond, suggesting small energy differences between rotamers and a marked preference for a single conformation of the ribose-phosphate system.

Molecular mechanics minimisation of the cAMP structure using COSMIC showed, by the small coordinate change on minimisation, that the parameters in the COSMIC force field could reproduce the crystal structure. Analysis with the COSMIC program MIN01, which used a pseudo-random technique for investigating conformational space, gave several sets of minimised structures within 15 kcal/mole of the global minimum energy conformation (Fig. 4). Each set, corresponding to flexing of the fused ribose-phosphate system, was separated from the next by about 4 kcal/mole. Within each set were conformations with an energy range of about 1 kcal/mole, resulting from the (relatively free) rotation about the riboside bond. The calculated global minimum energy conformation was similar to the crystal structure.

These pseudo-random calculations were complemented by investigations using the COSMIC SPIN01 program. Conformational change was forced by driving torsional angles and allowing

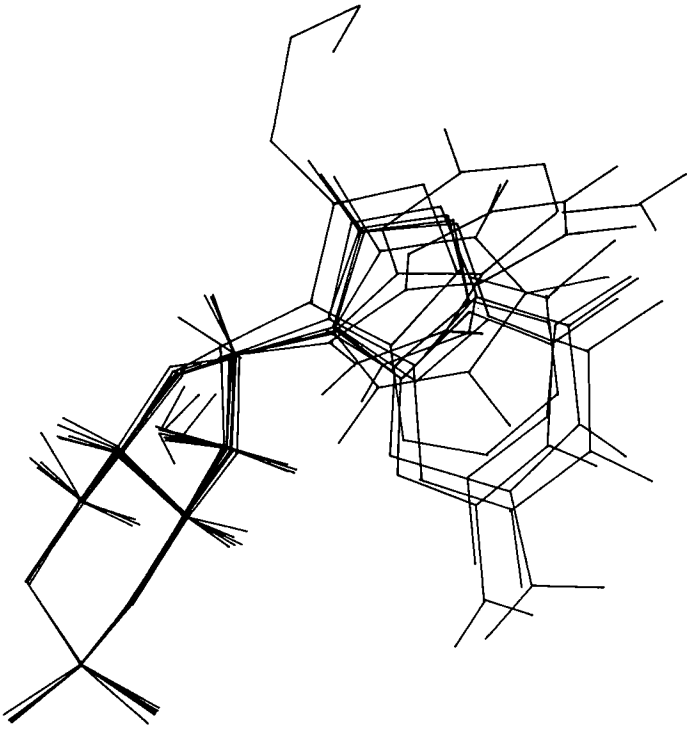

Fig. 2. Purine-3'5'-cyclic monophosphate structures from the Cambridge Crystallographic Database, overlaid to show the common phosphate ring conformations.

full structural relaxation, apart from the constrained torsional angle, at each torsional step. Three torsions were investigated, corresponding to rotation of the riboside bond, flexing of the ribose ring, and flexing of the phosphate ring. Both protonated (phosphoric acid) and anionic (phosphate) forms of cAMP and cGMP were investigated, on the assumption that the true charge state of the (solvated or enzyme-bound) phosphate anion lies somewhere between these two calculation extremes.

The profiles obtained for rotation at the riboside bond (Fig. 5) showed a relaxed barrier of 2–3 kcal/mole. The protonated forms of cAMP preferred torsional angles (C4–N9-ribose-O') of 40°–80° (syn); rotamers with angles 150°–250° (anti) were 0.8 kcal/mole higher in energy. The cAMP anion preferred 180°–250° (anti) over 20°–100° (syn) by about 2.3 kcal/mole. The latter result is consistent with other calculations and physical evidence which suggest that cAMP prefers to adopt an anti conformation [4,5]. For all cAMP species the main barrier to rotation was at about 130°. Although this is the result of non-bonded interactions, molecular relaxation methodology placed almost all of the barrier energy into angle bend. cGMP showed a lesser distinction between protonated and anionic forms—the angles 50°–70° (syn) were preferred over 150°–250° (anti) by 1 kcal/mole (protonated form) and 2.5 kcal/mole (anionic form), in agreement with calculations and physical evidence [5,6] showing that the syn form of cGMP is preferred.

Flexing of the ribose ring from the crystallographic position was accompanied in all species by an increase in energy. Although there was some evidence for a secondary minimum associated

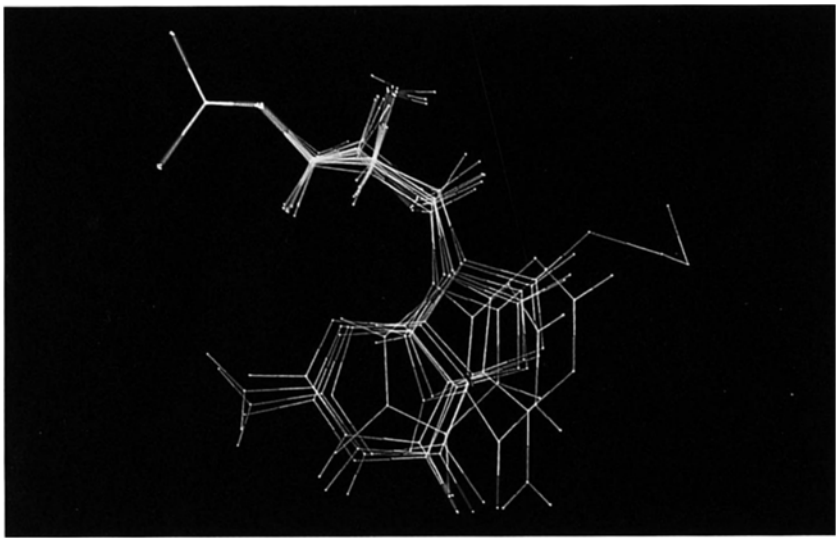

Fig. 3. Cyclic purine ribose phosphate structures extracted from the Cambridge Crystallographic Database, aligned to show the common ribose phosphate ring conformations (see Table 1). The major conformational variations are associated with rotation of the purine-ribose bond.

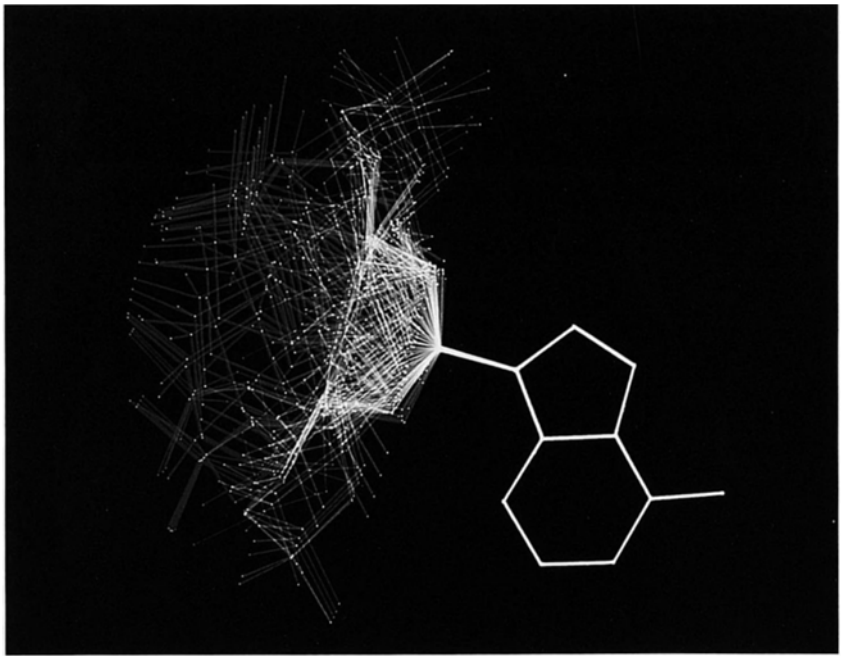

Fig. 4. The conformational space of cAMP derived from the COSMIC MIN01 algorithm. All conformations are superimposed on the purine moiety. The conformational energy ranges from the global minium, coded yellow, through red to blue at 15 kcals/mole above the global minimum. Flexibility is dominated by almost free (1 kcal/mole) rotation about the purine-ribose bond. Flexing of the fused 5/6 ring system requires about 4 kcals/mole (see text).

with this motion, in general the energy rose smoothly by 3–4 kcal/mole as the ring oxygen was flipped over the plane of the ring, a total torsional change of 40°.

Phosphate ring flexing in the anti forms of both cAMP and cGMP revealed a secondary minimum ('twist boat') 3–4 kcal/mole above the minimum ('chair') form, with a conversion barrier of about 7–8 kcal/mole. Calculations on the syn form of the cAMP anion gave a similar energy profile, but those on the syn form of cGMP showed a larger energy difference of almost 5 kcal/mole.

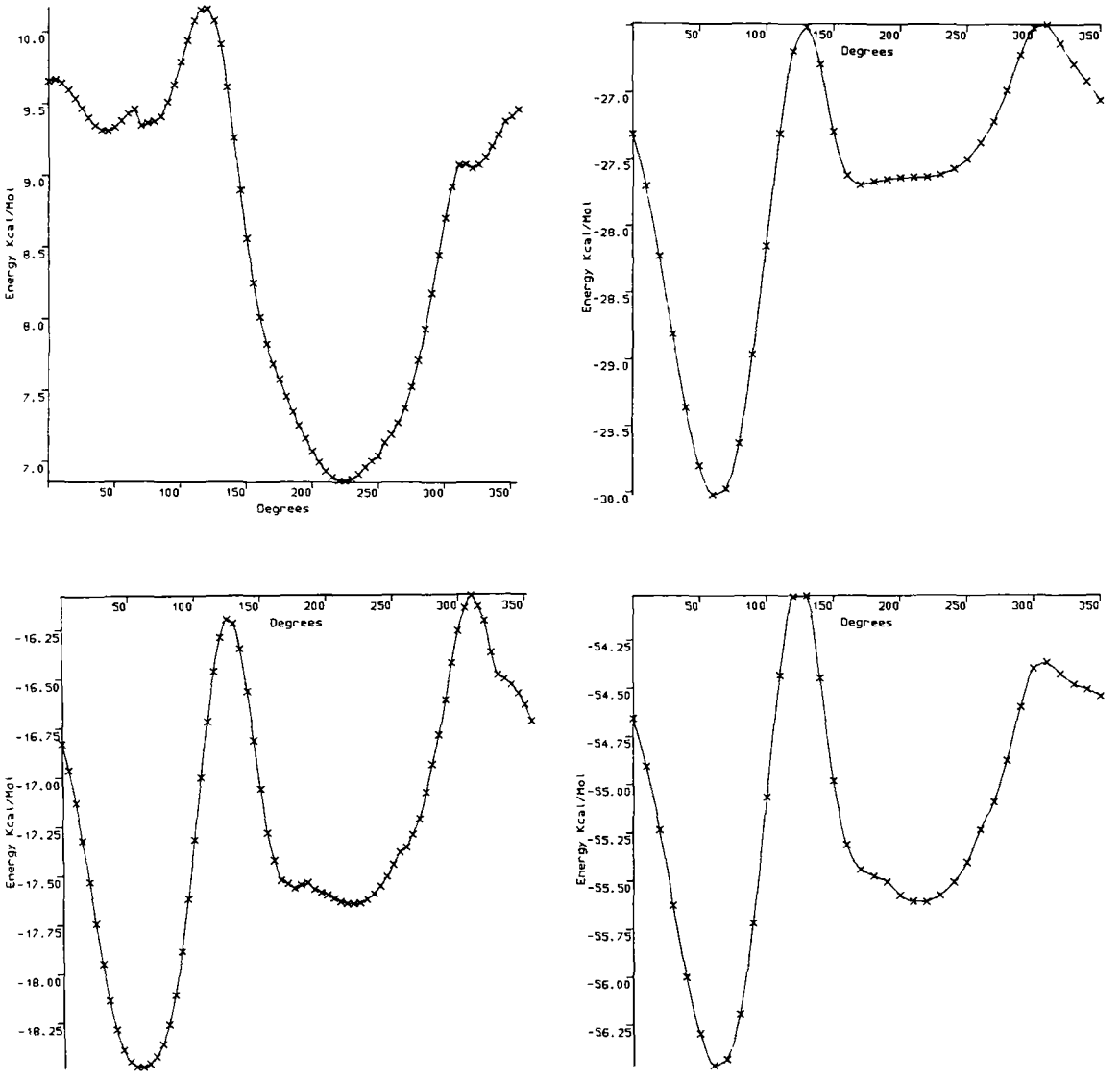

Fig. 5. Energy vs. riboside angle for the 'relaxed' rotation of cAMP (top left), cGMP (top right), equatorial protonated (phosphoric) cAMP (bottom left) and equatorial protonated (phosphoric) cGMP (bottom right).

Electronic Effects

On the assumption that the electronic nature of cyclic nucleotides is involved in selective recognition by PDE isozymes, the compounds identified in the crystal database search were examined for centres of solvation and counterion sites. Five 'binding sites' were identified and are listed in Table 1. Electrostatic minima associated with protonated (phosphoric) cGMP and cAMP were calculated using the COSMIC program NBMAP with CNDO atom-centered charges (Fig. 6). The calculation identified essentially the same binding sites as were found in the crystallographic study (Table 2).

Tautomers

Both guanine and adenine can undergo prototropic tautomerism, which modifies the electronic nature of the purine being presented for binding to the PDE enzyme. This has been shown to be of biological importance elsewhere [7]. Guanine shows (amongst others) keto, imino-enol and enol forms, and adenine the amino and imino forms. Adenine is structurally and electronically more similar to the enol tautomer of guanine than it is to the keto tautomer.

Tautomer energies were calculated using the ab initio program GAUSSIAN 80 with an STO–3G basis set allowing full atomic relaxation. The imino tautomer of adenine (dipole moment 5.00 Debye) was found to be 14.2 kcal/mole higher in energy than the amino tautomer (dipole moment 4.85 Debye), and thus is probably energetically inaccessible. However, the enol tautomer of guanine (dipole moment 1.83 Debye) was 8.0 kcal/mole lower in energy than its keto form (dipole mo-

TABLE 1
COUNTERION AND SOLVATION SITES OF CYCLIC NUCLEOTIDES FROM THE CAMBRIDGE CRYSTALLOGRAPHIC DATABASE

CCDB identifier		Counterion/solvation site[a]				
		1	2	3	4	5
AEADMP	(syn cAMP)	H_2O				
BEPRAP	(anti cIMP)			H_2O		H_2O
BIVJEV	(syn cGMP)		Ni+[b]			
CATTEW	(syn cIMP)		Cu+[b]		H_2O	
CATTIA	(syn cGMP)	H_2O[c]				
BULCOA	(cCMP)	H_2O				
NAAMPH10	(anti cAMP)	H_2O/Na+[b]				
SCGMPT10	(syn cGMP)		H_2O			

[a] Table headers:
1 Phosphate P=O oxygen (anion)
2 Purine 5-ring N(7)
3 Purine 6 ring N(3)
4 Purine C=O (Guanine, Inosine)
5 Ribose O–H
[b] '+' Signifies interaction with cation, and does not imply a valence state for the cation.
[c] This compound exhibits purine/phenanthroline 'stacking'.

TABLE 2
ENERGIES OF INTERACTION OF A PROTON WITH cAMP AND cGMP HETEROATOM SITES (FROM ELECTROSTATIC ISOPOTENTIAL MINIMA)

	cAMP	cGMP
Phosphate P=O	21.9	22.4
Ribose OH	9.4	6.4
Ribose cyclic O'	4.1	5.9
Purine N(1)	13.3	n/o
Purine N(3)	11.6	3.8
Purine N(7)	6.6	n/o
Guanine C=O	n/o	44.4

n/o = EIM not observed

ment 5.23 Debye). These calculations apply to the gas phase and do not take into account solvation effects, but it may be noted that there is some evidence for the low energy enol tautomer in solution studies of inosine [8]. Dipole moment may be as important a factor as energy in determining stability in polar environments. The effect of enzyme active site environment on prototropic tautomerism is unknown, but the energy differences between guanine tautomers are not large and it may be possible for the enzyme to invoke the tautomer required for binding.

In summary, of the two motions available to cyclic nucleotides, rotation about the riboside bond is the most accessible in energy terms, followed by flipping of the phosphate-containing, 6-membered ring (for which there is no evidence from crystallographic studies).

Clearly, elements of the reactive phosphate centre in both cAMP and cGMP are involved in binding to the PDE enzyme active site. It is unlikely that the purine can electronicallly modify the atoms of the RcP group, as these are effectively insulated by sp3 carbon atoms (CNDO calculations give charge differences between corresponding cAMP and cGMP Rcp atoms of less than 0.003). Differential recognition of cAMP and cGMP must therefore be achieved by either conformational effects and/or direct interaction associated with the purine.

Several potential binding groups have been identified in the study of electronic effects in cyclic nucleotides, and the following section describes attempts to use non-specific PDE enzyme inhibitore to determine which groups are commonly bound by this enzyme class.

MODELLING OF NON-SPECIFIC PDE INHIBITORS

Many inhibitors of PDE closely resemble purines, and it was reasonable to assume that at least some of these inhibitors bind at the purine site. However, the similar positioning of electronegative centres within the 6–5 purine and 6–5 RcP ring systems (apparent by overlaying the purine C(4) and C(5) with the ribose C(3') and C(4')) is a feature which must not be neglected.

Several known PDE inhibitors were built using COSMIC, and their NBMAP electronic isopotentials compared with those of adenine and guanine in an attempt to identify possible common binding sites (Figs. 7 and 8). The positions and energies of electrostatic minima are aligned to show (vertically) the overlay of two minima separated by a common distance. In some cases there are three or more minima, any pair of which could be aligned in this way.

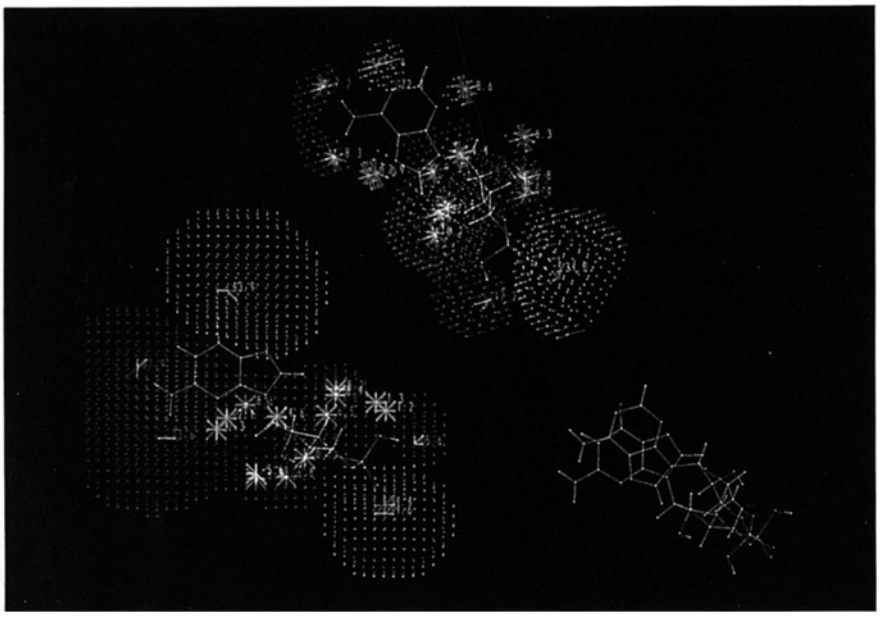

Fig. 6. Electrostatic isopotential contours and minima of cAMP (top) and cGMP (lower left). Interactions with H^+ are coloured blue (attractive 5 kcals/mole) and green (minimum energy wells recorded in kcals/mole). Interactions with OH^- are coloured red (attractive 5 kcals/mole) and orange (minimum energy wells recorded in kcals/mole). Inset to the lower right are the molecules overlaid according to electrostatic coincidence rather than steric correspondence (see Table 2).

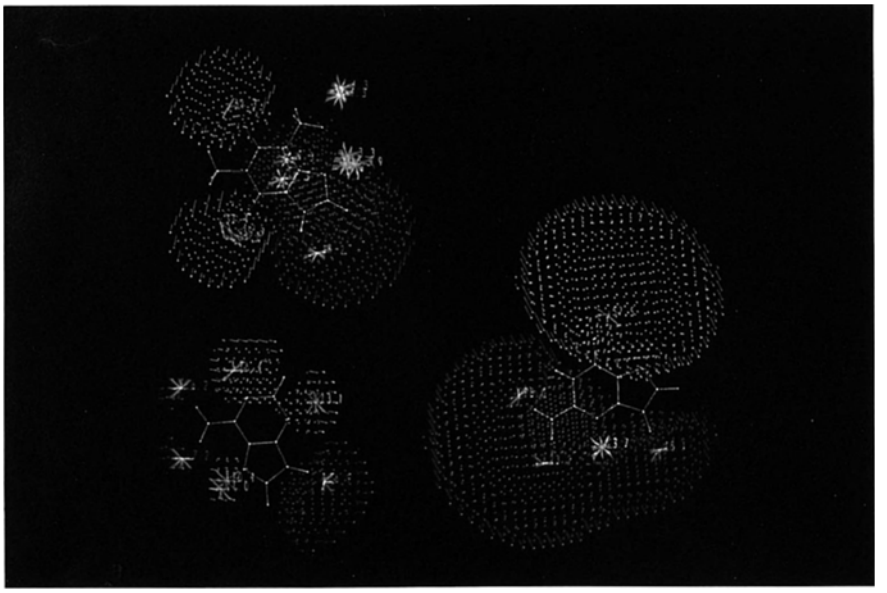

Fig. 7. Electrostatic isopotential contours and minima of theophylline (top left), adenine (lower left) and guanine (right). Colour coding and levels are as described for Fig. 6. The structures are aligned to show the vertical correspondence of two protonic (green) electrostatic minima. Theophylline and adenine show the correspondence of three (green) minima in a triangular arrangement.

Adenine showed three symmetrically-arranged minima. As oriented in Fig. 8, the phosphate group of anti-cAMP would extend to the lower right.

Guanine showed just two minima located on the carbonyl and on the N(3) nitrogen. The N(7) nitrogen may have hydrogen bonding capability (cf. CCDB study) but NBMAP merged the minimum associated with this atom into that generated by the cabonyl. Note that all minima of adenine and guanine can overlay, as well as the protons on the adenine amino group and guanine N(1). As oriented, the phosphate group of anti-cGMP extends to the lower right in a similar direction to that of cAMP.

Theophylline, IBMX and other purine diones gave three symmetrically-arranged minima, showing a number of possible two-point matches with the minima associated with adenine or guanine. Large side-chains may be extended in several directions, but some combinations appear from the available data to be mutually exclusive if affinity is to be retained. For example, large groups have been extended from any two of N(1), N(3), N(7) and C(8) [9] with retention of significant affinity. In addition, if N(3) has a bulky substituent then the 8-aza analogue shows enhanced affinity [10], and the best fit with adenine is by alignment of N(7)/N(8) with N(1) and C(6)=O with N(7) respectively, with the substituent extending to the lower right.

The identified two-point binding pattern can also be found within the many binding possibilities presented by etazolate and within a common fragment of many papaverine derivatives showing non-specific PDE inhibition.

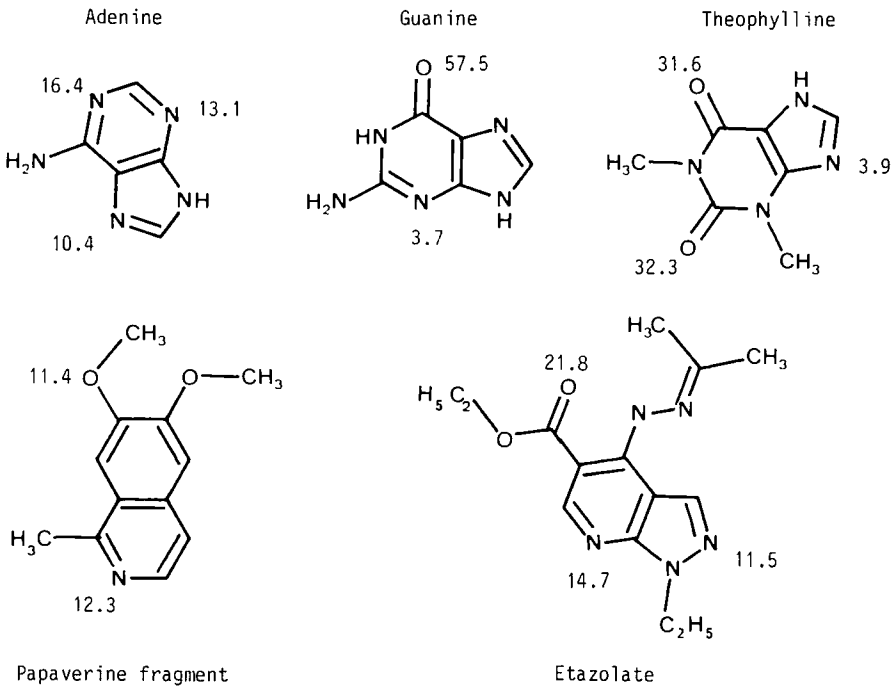

Fig. 8. Non-specific inhibitors of PDE III and their associated electrostatic isopotential minima (adenine, guanine, theophylline, papaverine fragment and etazolate).

These data suggest a rationale for the affinity of non-specific PDE inhibitors. As purine mimics they may bind to the purine recognition part of PDE isozymes via two electronegative atom positions which give rise to electrostatic minima overlaying two of the three minima in adenine (or guanine). The non-specific inhibitors modelled here can provide a similar electronic environment in this area without necessarily providing a similar steric environment. For example, theophylline derivatives with different substitution patterns can bind in different orientations to maintain a two-point electronic fit and still direct the side-chain bulk in a common direction.

As a consequence of the many binding possibilities available to purines it was noted that in one electronic overlay of cAMP and cGMP electrostatic complementarity was maintained around the purine with coincidence of equatorial phosphoryl groups (Fig. 9). This provides a possible binding model for isozymes which hydrolyse both cAMP and cGMP, if the isozyme has a pocket sufficiently large to accommodate both ribose ring orientations. However, other possibilities exist. These isozymes may bind the low energy enol tautomer of guanine, which has a similar electrostatic isopotential to that of adenine. Aternatively, binding may occour at electronically similar sites. Thus non-specific isozymes would bind at N(3) and/or N(7), while selective isozymes such as PDE III (which is selective for cAMP) would also bind at N(1) and/or the substituent at C(6).

MODELLING OF PDE III INHIBITORS

Empirical Analysis

Examples of the structurally diverse range of compounds showing PDE III inhibitory and/or inotropic properties are given in Fig. 10, arranged in groups of structural congeners. Initial modelling and minimisation demonstrated that all of these, except milrinone and the compounds in Group 2, had essentially planar preferred conformations. Milrinone gave a non-coplanar structure with an inter-ring torsion of approximately 50°, in good agreement with X-ray data [11], and the Group 2 compounds showed several low energy conformational minima. The positional correspondence of common potential binding groups of the compounds shown in Fig. 10 was sought using molecular graphics.

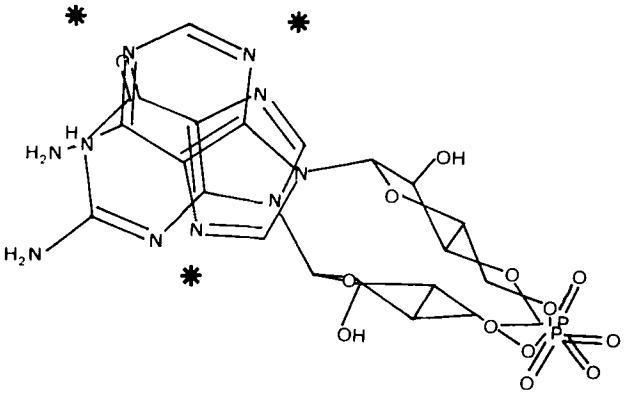

Fig. 9. cAMP and cGMP overlaid to match electrostatic isopotential minima positions (marked with an asterisk) on the purine and coincide equatorial phosphoryl groups.

GROUP 1

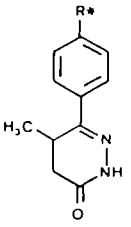

SK&F 93505 (R = *NH_2)
SK&F 93741 (R = *NHAc)
SK&F 94836 (R = *NHC(=NCN)$NHCH_3$
CI-930 (R = 1*-imidazolyl)

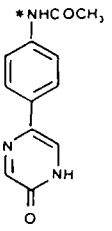

SK&F 94120

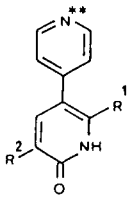

amirinone (R^1 = H; R^2 = NH_2)
milrinone (R^1 = CH_3; R^2 = CN)

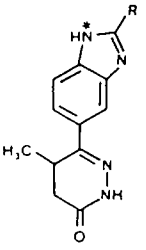

UD-CG 115BS (R = C_6H_4(4-OCH_3))
UD-CG 212 (R = C_6H_4(4-OH))

GROUP 2

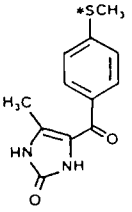

fenoximone

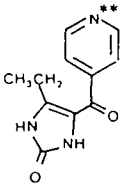

piroximone

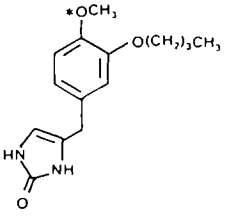

RO-20-1724

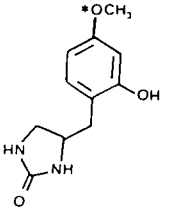

RO-20-2926

GROUP 3

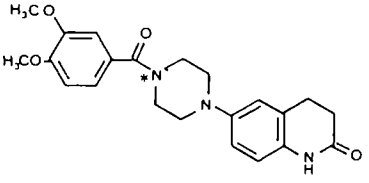

OPC-8212

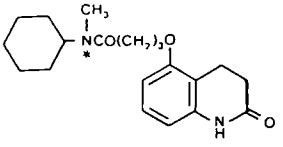

OPC-3689

GROUP 4

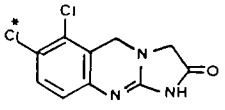

anagrelide

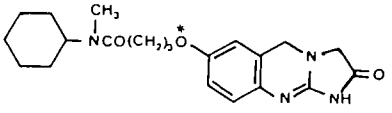

RS-82856

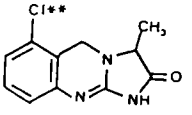

dazonone

GROUP 5

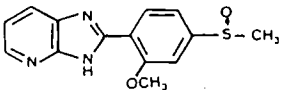

sulmazole

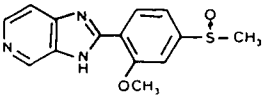

LY-17536

Fig. 10. Known PDE III inhibitors. IC_{50} data for compounds in this figure, where available, are given in Table 3 (1–14).

TABLE 3
STRUCTURE AND IC_{50} DATA FOR COMPOUNDS GIVEN IN TEXT AND REGRESSIONS

No.	Name	IC_{50} (μM)	Structure[a]	Substituents[a]		
				R^1	R^2	R^3
1	SK&F 93505	37.00	(A)	NH_2	CH_3	–
2	SK&F 93741	0.90	(A)	NHAc	CH_3	
3	SK&F 94836	1.05	(A)	$NHC(=NCN)NHCH_3$	CH_3	–
4	CI–914	3.72	(A)	1-imidazolyl	H	
5	CI–930	0.42	(A)	1-imidazolyl	CH_3	–
6	SK&F 94120	11.63	(C)	NHAc	–	–
7	Amrinone	51.80	(B)	NH_2	H	–
8	Milrinone	2.20	(B)	CN	CH_3	
9	UD–CG 115BS	1.34	(I)	4-(OCH_3)phenyl	CH_3	–
10	Fenoximone	8.01	(E)		–	
11	Piroximone	19.50	(F)	–	–	
12	Anagrelide	0.13	(G)	Cl	Cl	H
13	Dazonone	1.68	(G)	H	Cl	CH_3
14	Sulmazole	30% @ 100	(H)	–		–
15	SK&F 95422	2.23	(A)	$CONH_2$	CH_3	
16	SK&F 95484	0.33	(D)	6 (3 oxopyridazinyl)		
17	SK&F 95510	0.69	(A)	(P)	H	–
18	SK&F 95800	0.76	(U)		–	
19	SK&F 95654	0.41	(A)	1-(4 oxopyridyl)	CH_3	
20	SK&F 95629	2.48	(A)	(T)	H	
21	SK&F 95648	0.16	(A)	(Q)	H	–
22	SK&F 95630	0.87	(A)	(S)	H	–
23	SK&F 92538	61.70	(A)	NH_2	H	
24	SK&F 92600	7.13	(A)	NHAc	H	
25	SK&F 95294	0.53	(I)	CH_3	CH_3	–
26	SK&F 94934	4.27	(I)	CH_3	H	–
27	SK&F 92345	12.70	(A)	OMe	H	
28	SK&F 95811	2.05	(A)	1 (4 methylpiperidinyl)	H	[σ I subst]
29	SK&F 95827	5.09	(A)	1-(4-oxopyridyl)	H	–
30	SK&F 93639	6.38	(D)	NHAc		
31	SK&F 95640	3.99	(D)	1-(4 oxopyridyl)		
32	SK&F 95705	3.78	(J)	NHAc		
33	SK&F 95793	3.61	(J)	$NHC(=NCN)NHCH_3$	–	–
34	SK&F 95701	9.88	(J)	CN		–
35	SK&F 95702	5.35	(J)	$CONH_2$		
36	SK&F 95295	9.41	(J)	OMe		
37	SK&F 95742	7.46	(J)	NH_2	–	–
38	SK&F 93880	23.60	(C)	NH_2	–	
39	SK&F 94442	10.71	(C)	NO_2	–	
40	SK&F 95833	2.64	(C)	1 (4 oxopyridyl)		
41	SK&F 95181	10.30	(K)	NHAc	–	–
42	SK&F 95603	3.55	(K)	1-imidazolyl	–	–
43	SK&F 95157	8.38	(K)	$CONH_2$		
44	SK&F 95230	7.40	(K)	OMe		
45	SK&F 95641	30.00	(K)	NH_2	–	–
46	SK&F 94928	1.75	(L)	NHAc	–	–

47	SK&F 95132	2.93	(L)	$CONH_2$	-	-
48	SK&F 95190	8.79	(L)	NH_2	-	
49	SK&F 95778	1.96	(M)	NHAc	H	-
50	SK&F 95779	3.59	(M)	H	NHAc	-
51	SK&F 95764	0.49	(N)	-	-	-
52	SK&F 95807	3.90	(O)	-	-	-
53	SK&F 95672	1.08	(A)	(R)	H	-
54	SK&F 93403	22.80	(D)	NH_2	-	-

[a] For structures and substituents shown in parenthesis see Fig. 13.

For all azinones in Groups 1–4, except amrinone, milrinone, piroximone and dazonone, overlay of the cyclic amide groups of minimised structures brought into correspondence an electronegative atom (marked * in Fig. 10) attached (except in the case of Group 3 compounds) directly to an aromatic ring. A good fit (distance RMS < 1.0) was obtained in all cases. A similar result was obtained for the excluded compounds when overlaid in the same manner, but the electronegative atom (marked ** in Fig. 10, frequently forming part of a ring system) was positioned closer to the azinone cyclic amide. In addition the methyl groups in SK&F 93505 and 94836, CI-930, UD-CG 115 and 212, fenoximone, dazonone and the ethyl group in piroximone were found to overlay.

The compounds in Group 5 showed poor and ambiguous fits with either of the above models. However, it is known that the PDE III inhibitory properties of at least one of these, sulmazole, are weak, and inotropic action is achieved through additional mechanisms [12]. The compounds in this group were therefore discarded from further analysis.

Electrostatic Modelling

Although these empirical analyses demonstrated the commonality of certain electronegative substituents, the very high affinity of compounds having a longer substituent attached through a nitrogen atom (e.g. Table 3 No. 2), or attached through carbon (e.g. Table 3 No. 15), implied that an optimal interaction probably occurs through a centre at a greater distance from the cyclic amide group. To compare the binding options of inhibitors against those of the natural substrate, a range of azinones known to have PDE III inhibitory activity were modelled using COSMIC. Atom-centered charges were calculated by the CNDO method and the program NBMAP was used to calculate electrostatic potentials and their associated minima. Despite differences in azinone ring structure, isopotential plots were remarkably uniform and the site of deepest electrostatic isopotential minimum (EIM) was always the carbonyl of the cyclic amide structure.

cAMP, extracted from the Cambridge Crystallographic Database, was similarly treated. Although more complex, the isopotential plot obtained showed the phosphate group as the centre of electronic charge. Moreover, the isopotential in this region was similar in extent and magnitude to that found in the azinone rings, suggesting that the important phosphate group is mimicked at the active site by the ring amide carbonyl of inhibitors (Fig. 11).

Comparison of the conformational space of cAMP with that of SK&F 93505, with the phosphate and amide groups overlaid, revealed one cAMP conformer (syn) where amine-amine overlay was possible, and one (anti) cAMP conformer in which the SK&F 93505 amino substituent

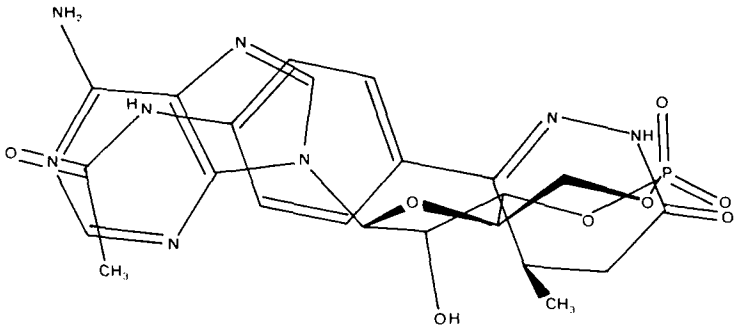

Fig. 11. Overlay of cAMP with SK&F 93741 (see text).

approached N(1) of adenine. When this analysis was extended to the wider range of inhibitors, it was comparisons with the anti rotamer which gave the more consistent explanation of the effect of phenyl substituent structure on affinity. PDE III inhibitors showing high affinity (e.g. SK&F 93741) were found to show a common EIM related to the atom centre overlaying the largest EIM on the adenine moiety of cAMP, N(1). Compounds showing lower affinity, e.g. SK&F 93505 and SK&F 95629 (Table 3 No. 20), had EIM locations which extended away from the cAMP N(1) centre.

There was some evidence for a second potential binding site in SK&F 95648 (Table 3 No. 21), anagrelide and others. In anagrelide the EIM was centered between the two chlorine atoms; in SK&F 95648 a similar EIM was related to a carbonyl oxygen; in both cases the EIM overlaid with the second largest EIM of adenine associated with N(3). The EIMs of compounds of the 'short' series as defined by the empirical analysis (i.e. amrinone, milrinone, piroximone and dazonone) fell well short of the EIM on cAMP N(1) but were found to overlay that of cAMP N(3).

Further examination of the overlay of cAMP and SK&F 93505 (similar to Fig. 11) for factors explaining the greater than 100-fold difference in the inhibitory potency of SK&F 93505 enantiomers [13], revealed that different environments were possible for the chiral axial 5-methyl group. In the (*R*)-enantiomer the methyl overlaid a similarly hydrophobic region in the ribose-phosphate ring junction, whereas in the (*S*)-enantiomer the 5-methyl group entered the hydrophilic ribose hydroxyl region. On this basis it was predicted that the (*R*)-enantiomer of SK&F 93505 would show the higher affinity. This was later confirmed by X-ray crystallography [14]

Initial binding of a phosphate-mimicking cyclic amide group, followed by optimal fitting of electronegative and hydrophobic centres to accessible sites in the purine and ribose areas of the active site, could qualitatively explain the affinity of azinone-based PDE III inhibitors. However, several features of quantitative action required resolution. Principally these were the differences of affinity arising from changes of structure in the azinone ring and the phenyl substituent.

Azinone relative affinities are ordered according to: pyridazinone > pyrazinone = pyridinone > 1,3-pyrimidinone. Calculations of charge, dipole moment and molecular orbital coefficients around the cyclic amide demonstrated a remarkable uniformity across this series and could not explain the relative affinities. It is therefore likely that differences in affinity arise from the

manner in which other features of the azinone ring either interact directly at the binding site, or influence the primary carbonyl binding.

The Phenyl Substituent - Vector Modelling

Despite prolonged commercial interest in inotropic vasodilators acting through a PDE III mechanism, to our knowledge no successful analysis of substituent properties and affinity in phenylazinones has been reported. In our hands regression of functions of phenyl ring substituent volume, lipophilicity, field effect and resonance against affinity gave poor or non-existent correla-

TABLE 4
DATA USED IN REGRESSION OF SET I

Vector[a]			Relative affinity[b]						Substituent
			Ring system					Average	
No.	d	Θ	(A) ($R^2=CH_3$)	(A) ($R^2=H$)	(D)	(J)	(C)		
1	0.40	49	1.00 (2)	1.00 (24)	1.00 (30)	1.00 (32)	1.00 (6)	1.00	NHAc
2	0.10	55	1.16 (3)			0.85 (33)	–	1.05	$NHC(=NCN)NHCH_3$
3	0.30	32	0.46 (5)	0.52 (4)	–	–	–	0.49	1-imidazolyl
4	2.05	9	–	–	–	2.61 (34)	–	2.61	CN
5	1.50	20	2.50 (15)	–	–	1.42 (35)	–	1.96	$CONH_2$
6	2.80	31[c]	0.58 (25)	0.60 (26)		–	–	0.59	3,4 NH–CH=N–[d]
7	2.50	52	–	1.78 (27)	–	2.48 (36)	–	2.13	OCH_3
8	2.80	25		8.60 (23)	3.60 (54)	1.97 (37)	2.02 (38)	3.92	NH_2
9	1.80	38		–	–	–	0.92 (39)	0.92	NO_2
10	0.40	93		0.28 (28)			–	0.28	N-piperazinyl
11	2.30	45	0.45 (19)	0.71 (29)	0.62 (31)	–	–	0.59	1-(4-oxopyridyl)

[a] Vectors are for the substituents considered in Fig. 12. d = distance between closest substituent lone pair and cAMP (A) lone pair. Θ = angle between substituent and cAMP lone pair vectors.

[b] Substituent relative affinities for ring systems A, D, J and C (see Fig. 13) are given as ratios (NHAc = 1) calculated from IC_{50} data for the compounds in Table 3 (compounds numbers are indicated in parentheses immediately below each relative affinity).

[c] Vector 6b has Θ = 50.

[d] Benzimidazole, ring system (I) in Fig. 13.

TABLE 5
DATA USED IN REGRESSION OF SET 2

Substituent	Ring system K			Ring system L		
	Vector		Relative	Vector		Relative
	d	Θ	affinity	d	Θ	affinity
NHAc	0.8	48	1.00	0.7	52	1.00
NH_2	3.0	12	2.91	2.9	19	5.02
OMe	2.7	40	0.72	–	–	–
$CONH_2$	1.7	10	0.81	1.6	15	1.67
1-imidazolyl	0.8	12	0.34	–	–	–

Substituent relative affinities in ring systems K and L (see Fig. 13) are given as ratios (NHAc = 1) calculated from IC_{50} data for compounds (40–49) in Table 3. d = distance between closest substituent lone pair and cAMP (A) lone pair. Θ = angle between substituent and cAMP lone pair vectors.

tions for all data sets examined. An alternative approach using the overlay data generated in the EIM study was therefore considered.

COSMIC was used to identify energy-minimised conformers of the phenylazinones shown in Table 3, then lone pairs were added to the heteroatoms. All lone pairs were found to lie close to, or be readily constrained to lie in, the plane of the phenylazinone system. Vectors representing the substituent lone pairs with (arbitrary) unit length were then compared with the purine lone pair vectors of anti-cAMP when overlaid on EIM's as shown in Fig. 11. To simplify analysis of the results the vectors were divided into the three sets shown in Tables 4–6.

Set 1 (Fig. 12) includes structures in which the axes of the phenyl and azinone rings are colinear ('linear systems'). Inspection revealed that at least one vector of substituents conferring a high level of affinity could be found close to the vectors A or B, which describe the lone pairs of the

TABLE 6
ADDITIONAL DATA USED FOR REGRESSION OF SET 3 WITH SET 1

Vector		Relative	Compound
d	Θ	affinity	(Table 3)
0.2	49	0.05	(16)
2.3	45	0.59	(19)
2.0	40	0.76	(17)
1.0	3	0.18	(21)
1.1	40	0.08	(51)
0.4	43	1.20	(53)
0.3	23	0.61	(52)
0.3	39	0.97	(22)

Substituent relative affinities are calculated from IC_{50} data given in Table 3 as a ratio to that of the NHAc substituted compound of the ring system considered. d = distance between closest substituent lone pair and cAMP (A) lone pair. Θ = angle between substituent and lone pair vectors.

N(1) and amino groups of cAMP respectively. In contrast, substituents conferring lower levels of affinity showed no lone pair options in these areas.

Set 2 includes structures in which the axes of the upper and lower rings are not colinear, and rotation at the inter-ring bond is impossible ('angular systems'). Vectors associated with compounds showing high levels of affinity were found to cluster almost exclusively around vector A, corres-

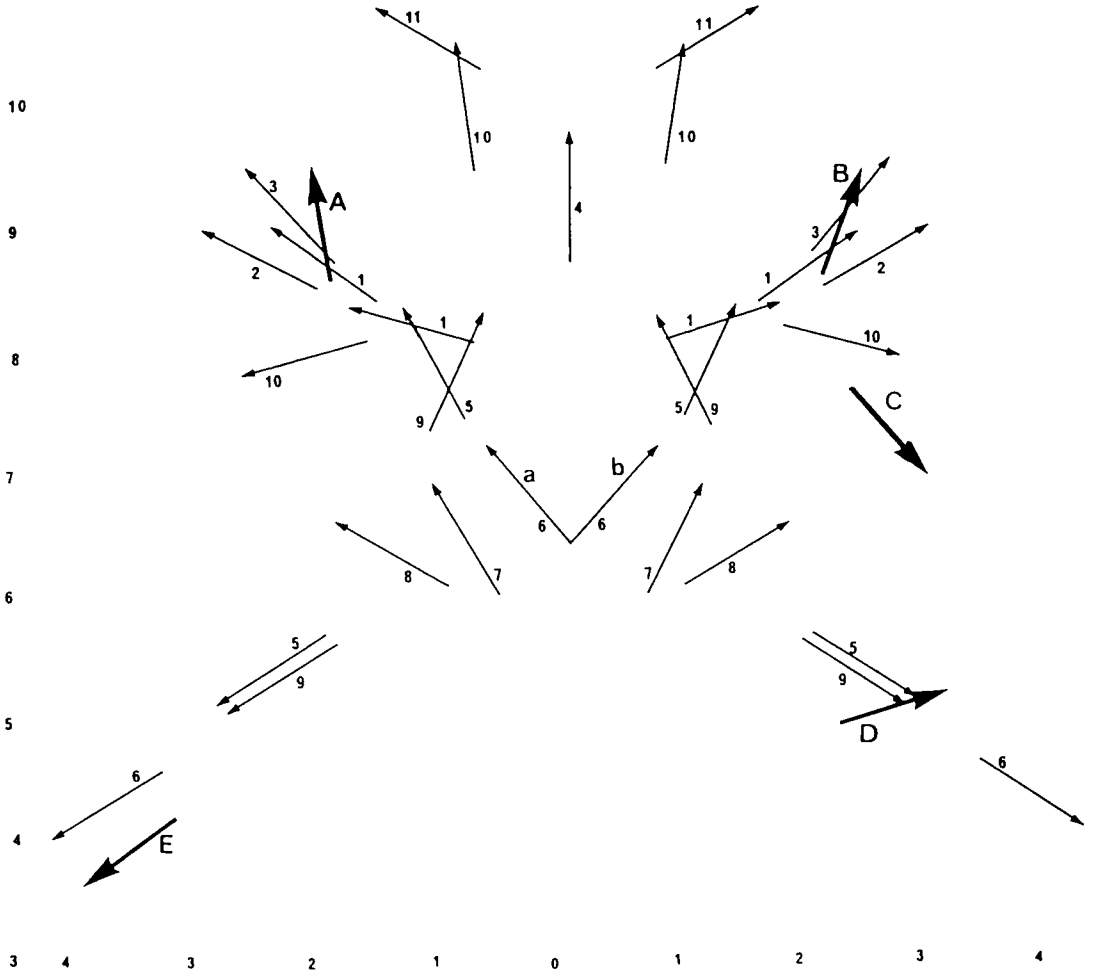

Fig. 12. Lone pair options of linear systems (Set 1). Vectors (1–11) representing substituent lone pairs are plotted in the X–Y plane with those of cAMP as overlaid in Fig. 11. In the absence of proton affinity data, each vector is given an arbitrary length of unity, its origin marking the actual position of the lone pair and its direction being the heteroatom-lone pair axis. Where alternative minimised forms are available for inhibitors, all options are plotted (marked for substituent 6 as a,b). Vectors shown are for the following substituents: (1) NHAc; (2) NHC(=NCN)NHCH$_3$; (3) 1-imidazolyl; (4) CN; (5) CONH$_2$; (6) 3,4-NH–CH=N– (benzimidazole); (7) OCH$_3$; (8) NH$_2$; (9) NO$_2$; (10) N-piperazinyl; (11) 1-(4-oxopyridyl). All distances shown are relative to C(6) of a pyridazin-3[2H]-one drawn with the C(3)–C(6) axis at $x=0$ and C(6) at $y=0$. The bold vectors A,B,C,D and E represent lone pairs on cAMP heteroatoms N(1), N(NH$_2$), N(NH$_2$ rotated), N(7) and N(3) respectively.

ponding to the N(1) lone pair of cAMP and the position of deepest electrostatic isopotential minimum on the cAMP purine.

Set 3 consists of linear compounds with high affinity and a large number of binding options. In agreement with the findings for Sets 1 and 2, at least one lone pair option for each compound was found close to cAMP vector A.

The Phenyl Substituent – Regression

Vector plots such as Fig. 12 confirmed the importance of the N(1) binding site first demonstrated by EIM modelling. Numerical analysis of these vector data further showed that the relative level of affinity associated with each substituent depends to a large degree on the distance and alignment of one of its lone pair vectors relative to the cAMP N(1) vector.

To carry out this numerical analysis, it was necessary to obtain a measure of substituent affinity independent of the azinone ring system to which the substituents are attached. Thus, relative affinities of substituents were calculated from the IC_{50} data in Table 3 by assigning the acetamido group a relative affinity of unity for each azinone ring system. Substituent relative affinities for data set 1 (Table 4) show little spread between azinone systems, confirming the validity of the exercise. Tables 5 and 6 show similar substituent relative affinities for data sets 2 and 3 respectively. These values (averaged in the case of Set 1) were used in regressions against functions of d, the distance between substituent and cAMP vector A lone pairs, and θ, the angle between these vectors.

The results of the regressions are summarised in Table 7 and the following points can be made:

In Set 1 (Fig. 12 and Table 4) the benzimidazole vector 6b showed better regression than vector 6a (comparing Eqs. c and d with a and b in Table 7), but the benzimidazole substituent remained an outlier showing unusually large affinity regardless of the lone pair vector chosen. Exclusion of this point gave improved correlations (Table 7; Eqs. e and f), the principal outlier then being the amino substituent, which had shown the greatest spread before averaging.

In Set 2 (Table 5) separate analyses of 4a–methyl– indenopyridazinones (Table 7; Eqs. i and j) and 6a–methylindeno–thiadiazinones (Table 7; Eqs. k and l) gave regressions which agreed with the results of Set 1, but which were of poor statistical validity.

The compounds in Set 3 showed a narrow range of high affinity and no satisfactory regression could be carried out. Regression of Sets 1 and 3 combined gave poorer correlations (Table 7; Eqs. o and p) than Set 1 alone. This was possibly due to the greater range of substituent size and polarity of compounds in Set 3, or the effects of further substituent interaction. It is important to note that examples (3), (5), and (7) in Set 3, and the benzimidazole (6) in Set 1, showed additional alignments at the cAMP vector E (corresponding to cAMP N(3)) and exhibit higher affinity than predicted.

Regressions on d or d^2 for Set 1 (Table 7; Eqs. g and h), and Sets 1 and 3 combined (Eqs. m and n), showed that relative affinity regresses largely on distance. However, the improved regressions obtained when an angular term was considered suggested that binding at the N(1) site involves some directionality and is not purely electrostatic.

DISCUSSION

Regression analysis has suggested that the relative affinity of a series of substituted phenylazin-

TABLE 7
REGRESSIONS OF ACTIVITY ON LONE-PAIR DISTANCES (d) AND ANGLES (Θ) ACCORDING TO (RELATIVE AFFINITY) = A * f(d,Θ) + B

Eq.	A				B	Statistics of fit			
	d	d^2	d cos(Θ)	$(d \cos(\Theta))^2$	coef	r^2(%)	S	F	n
a			0.767		0.581	37.4	0.861	7.03	11
b				0.306	0.816	35.1	0.877	6.46	11
c			0.948		0.412	53.9	0.739	12.78	11
d				0.449	0.590	66.7	0.627	21.27	11
e			1.090		0.407	77.1	0.527	31.36	10
f				0.429	0.603	87.9	0.383	66.64	10
g	0.876				0.376	62.1	0.679	15.73	8
h		0.327			0.649	70.2	0.602	22.23	8
i			0.775		−0.079	41.5	0.774	3.81	5
j				0.257	−0.307	65.5	0.595	8.52	5
k			1.750		−0.190	76.9	1.038	7.61	3
l				0.775	−0.079	96.1	0.429	49.44	3
m	0.475				0.437	18.4	0.884	5.05	19
n		0.179			0.589	22.1	0.864	6.09	19
o			0.750		0.310	32.6	0.803	9.71	19
p				0.404	0.419	50.4	0.689	19.31	19

Key to Equations:
a,b Set 1, Benzimidazole vector 6a included.
c,d Set 1, Benzimidazole vector 6b included.
e,f,g,h Set 1, Benzimidazole excluded.
i,j Set 2, 4a-methyl-indeno-pyridazinones (ring system K, Fig. 13).
k,l Set 2, 6a-methyl-indeno-thiadiazinones (ring system L, Fig. 13).
m,n,o,p Sets 1 and 3 combined.

one inhibitors can be explained in terms of interaction of a substituent lone pair at the adenine N(1) site. However, this analysis could not be extended to include 'short' compounds (pyridylpyridinones such as amrinone and milrinone). Any attempt to explain their affinity in terms of an interaction at the N(1) binding site would have to invoke long hydrogen bonds or conformational changes in the binding site beyond the limits of a physically reasonable model.

A consideration of binding energies showed that those of amrinone and milrinone greatly exceed the values obtained by adding individual functional group binding energies [16], whereas extended structures, such as SK&F 95484 and SK&F 95800, showed smaller differences between calculated and observed values (see Table 8). This suggested that the 'short' inhibitors are bound more efficiently than the 'long' inhibitors and should show a better match with their accessible binding sites. Yet the pyridyl lone pairs of the pyridylpyridinones are about 3Å further from the N(1) binding site than the relevant vectors of SK&F 95484 and 95800.

It is more likely that inhibitors of the 'long' and 'short' series are showing different binding modes in the purine-accepting region of the PDE III isoenzyme, their respective interactions being at the N(1) and N(3) binding sites identified by EIM modelling. This dual model of binding is also

TABLE 8
COMPARISON OF OBSERVED AND CALCULATED BINDING ENERGIES OF SELECTED COMPOUNDS

Compound	Observed binding energy [a]	Calculated binding energy [b]	Difference
Milrinone	8.33	0.1	8.2
Amrinone	6.46	-0.7	7.2
SK&F 92538	6.35	-0.5	6.9
SK&F 95800	8.96	5.2	3.8
SK&F 95484	9.46	6.0	3.5

[a] kcal/mole; calculated from observed binding constant K_i using the equation $\Delta G = -RT\ln(K_i)$. K_i is derived from IC_{50} data shown in Table 3, using the Cheng-Prusoff [15] equation: $K_i = IC_{50}/(1 + D/K_d)$ in which D is the concentration of labelled ligand and K_d is its dissociaton constant. In all cases $D = 1.0$ and $K_d = 0.6M$.

[b] kcal/mole; calculated by summation of functional group contributions and subtraction of entropy related terms as described in Ref. 16.

more consistent with the apparent requirement for coplanarity in the 'long' inhibitors [17–19] whereas high-affinity compounds in the bipyridyl series often possess non-planar low energy conformations [11].

High-affinity compounds acting at the N(1) site show a preference for coplanarity and have either a rigid coplanar ring system (e.g. the tricyclic systems G, J, K and L in Fig. 13), or a non-rigid system in which resonance between rings forces coplanarity (e.g. the phenyldihydropyridazinones shown in Fig. 10, Group 1). However, further constraint (by the addition of another ring) of an already coplanar structure does not lead to higher affinity (cf. Table 3 Nos. 2,31; 1,36; and Ref. 19). Further, non-coplanarity of the rings of 'short' compounds (acting at N(3)) does not *per se* lead to low affinity (cf. milrinone). It may be concluded that coplanarity of the azinone ring with the extended purine-mimicking substituent of 'long' inhibitors is the critical requirement for effective interaction at the N(1) site, rather than coplanarity of the entire structure. This usually requires coplanarity of the intervening ring.

Rotations about the main axis of the arylazinone moieties of PDE III inhibitors would have little effect on the electrostatic interaction at the phosphate site. The different planarity requirements of the 'long' and 'short' series are thus probably related to the differing positions of their purine-mimicking groups relative to this axis.

Phenyldihydropyridazinones and 5–methyldihydropyridazinones both require coplanarity for optimal binding. Affinity in these series is modulated by individual phenyl ring substituents in a parallel manner (see Refs. 18,19 and Table 4). Clearly, the 5-pseudo-axial methyl substituent is being accommodated to reinforce binding without disturbing the interactions of other groups. Similar compounds with larger axial groups (e.g. ethyl) or a 5-methyl group lying in the plane of a pyridazinone ring are known to have lower affinity than the parent compounds [18]. The presence of these larger or misplaced 5-substituents would be expected to force rotation of the azinone about its main axis. In the absence of any compensating bond rotations elsewhere in the molecule, the off-axis purine-mimicking group would be displaced from its optimal binding position.

In contrast, 4-pyridylpyridinones binding at the N(3) site interact through groups lying in the

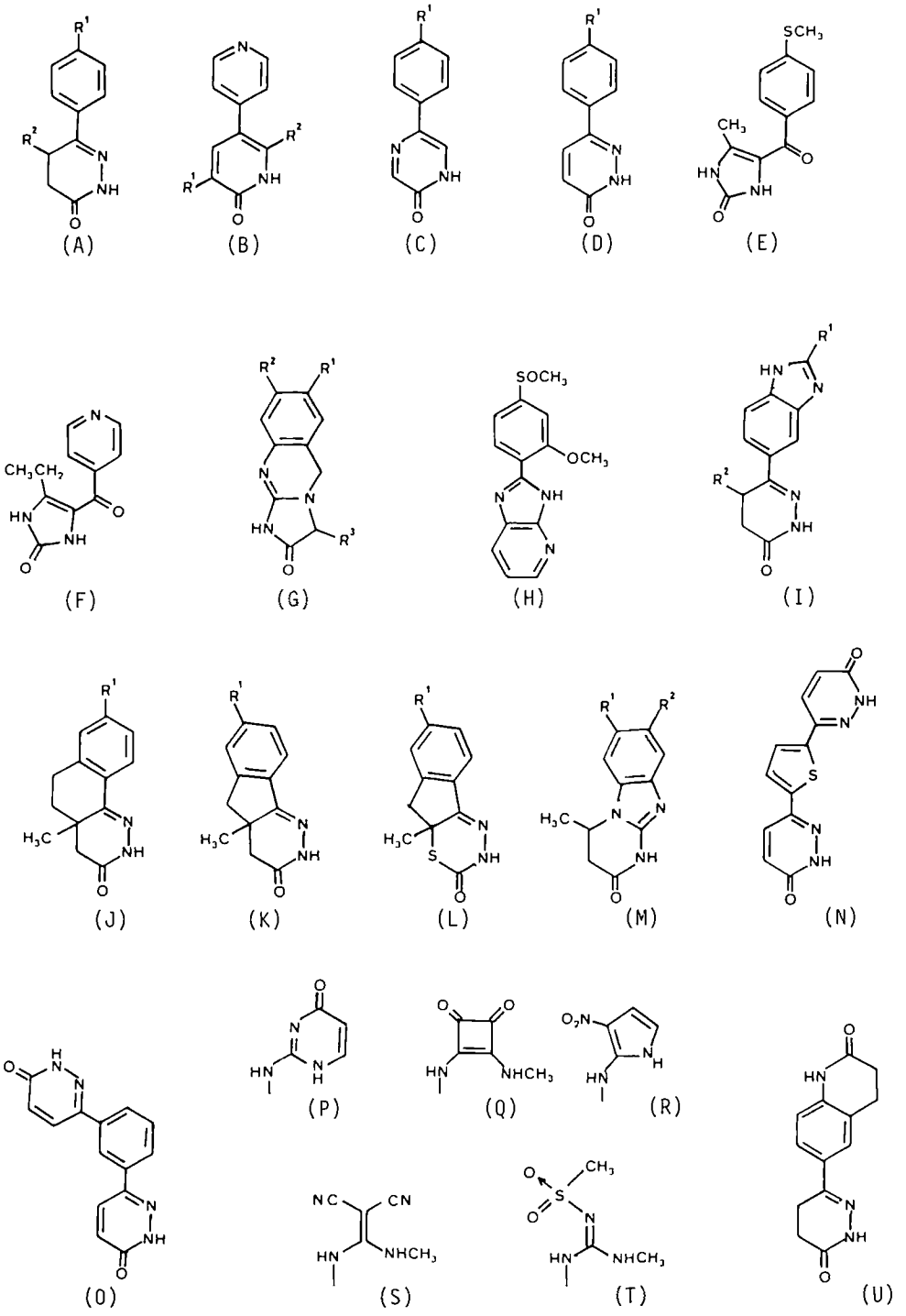

Fig. 13. Structural templates for the compounds listed in Table 3.

major axis of the molecule. Rotations about the major axis would, therefore, have little effect on binding. The 20-fold greater affinity of milrinone over amrinone can be explained by the regiospecific interaction available for its methyl group at the hydrophobic binding site identified for SK&F 93505. This conclusion is in good agreement with reports [11] that the affinity difference between amrinone and milrinone arises from the presence of a methyl group in the latter rather than from any other difference in substitution. Their binding energy difference (approx. 2 kcal) is similar to that of similarly related pairs in Table 3 (e.g. Nos. 1, 23; 2, 24; 5,4).

The binding of 'short' inhibitors is thus less critical than that of 'long' inhibitors since the binding groups lie along the axis of the molecule. The greater levels of affinity seen in the 'long' series probably reflect a greater binding energy at the N(1) site. However, it is possible that some 'long' compounds derive exceptionally high affinity by interacting at both purine sites. This would be consistent with the study of non-specific inhibitors presented earlier.

In summary, the overall picture to emerge from this study is that inhibitors showing a high degree of specificity for the type III isoenzyme [20] are characterised by the presence of an azinone moiety, the amidic carbonyl of which makes a crucial and powerful interaction at the phosphate-binding site. Further electronegative centres are able to interact at positions corresponding to the N(1) and/or N(3) domains of anti-cAMP when overlaid as shown in Fig. 11. Although the minor contributor to overall binding, this purine-mimicking substituent is important in determining PDE III inhibitory activity and selectivity. High levels of affinity are shown by inhibitors which are bound at N(1) and have preferred conformations in which the azinone system and electronegative substituent atom lie in the same plane. Lower but useful levels of affinity are shown by compounds which bind at the N(3) site only. In these, planarity is of little importance. A methyl group at the position shown in Fig. 11 enhances binding to the extent of 1–2 kcal/mole in all cases.

CONCLUSION

Computational chemistry and molecular graphics have been combined with both physical and biological data to study the interactions of the phosphodiesterase enzyme with natural substrates and synthetic inhibitors. Specific binding points (defined by points at which the electrostatic interaction of a proton with the target are most stable) have been used to give a consistent picture of the binding requirements of both non-specific and specific inhibitors. These points are situated on or beyond the van der Waals surface and broadly consist of: (a) a single, large point corresponding with an anionic group and probably representing a primary link; (b) a variable set of points associated with the purine of the natural substrate which are likely to represent the secondary binding area and which are able, in appropriate combination with (a), to define specificity; and (c) a third point which (by hydrophobic interaction) can further affect potency by its (chiral) influence.

The complementary study by lone-pair construction and regression analysis reaches essentially the same working rules for structure-activity and provides quantitative support for the hypothesis.

It is notable that structural overlay in this particular case seems to be of less significance than electronic overlay. Indeed, structural comparisons have misled us at times. The main driving force for recognition and orientation are undoubtedly the coulombic interactions which have been the subject of these studies. However, steric influences play their part in the bound state.

Compounds designed to access the more effective N(1) site demonstrated by these studies were found to show the expected high potency.

ACKNOWLEDGEMENTS

This work would have been impossible without the support of many colleagues at Smith Kline & French Research. We are particularly indebted to Dr. W.J. Coates for constructive advice and criticism. We would also like to acknowledge the valuable contributions of Ms. S.J. Bakewell, Dr. J.C. Emmett, Mr. S.T. Flynn, Dr. W. Howson, Mr. R. Novelli, Mr. H.D. Prain, Mr. M. Reeves and Dr. M. Saunders.

REFERENCES

1 Beavo, J.A., Hansen, R.S., Harrison, S.A., Hurwitz, R.L., Martins, T.J. and Mumby, M.C., Mol. Cell. Endocrinol., 28 (1982) 387–410.
2 Vinter, J.G., Davis, A. and Saunders, M.R., J. Comput.-Aided Mol. Design, 1 (1987) 31–51.
3 Reeves, M.L., Leigh, B.K. and England, P.J., Biochem. J., 241 (1987) 535–541.
4 Fitzakerley, G.V., Russell, J.C. and Wolfe, M.A., Eur. J. Biochem., 76 (1977) 601–605.
5 Yathindra, N. and Sundaralingam, M., Biochem. Biophys. Res. Commun., 56 (1974) 119–126.
6 Druyan, M.E., Sparagana, M. and Peterson, M.E., J. Cycl. Nucleotide Protein Phosphorylation Res., 2 (1976) 373–377.
7 Topal, M.D. and Fresco, J.R., Nature, 263 (1976) 285–289.
8 Chenon, M.T., Pugmire, R.J., Grant, D.M., Panzica, R.P. and Townsend, L.B., J. Am. Chem. Soc., 97 (1975) 4636–4642.
9 Kramer, G.L., Garst, J.E., Mitchell, S.S. and Wells, J.N., Biochemistry, 16 (1977) 3316–3321.
10 Coulson, C.J., Ford, R.E., Lunt, E., Marshall, S., Pain, D.L., Rogers, I.H. and Wooldridge, K.R.H., Eur. J. Med. Chem., 9 (1974) 313–320.
11 Robertson, D.W., Beedle, E.E., Swartzendruber, J.K., Jones, N.D., Elzey, T.K., Kauffmann, R.F., Wilson, H. and Hayes, J.S., J. Med. Chem., 29 (1986) 635–640.
12 Hertzig, J.W., Feile, K. and Ruegg, J.C., Arzneim.-Forsch. Drug Res., 31 (1981) 188–191.
13 Novelli, R. and Reeves, M.L., Unpublished.
14 Prout, C.K., Unpublished.
15 Cheng, Y.-C. and Prusoff, W.H., Biochem. Pharmacol., 22 (1973) 3099–3108.
16 Andrews, R.R., Craik, D.J. and Martin, J.L., J. Med. Chem., 27 (1984) 1648–1657.
17 Bristol, J.A., Sircar, I., Moos, W.H., Evans, D.B. and Weishaar, R.E., J. Med. Chem., 27 (1984) 1101–1103.
18 Sircar, I., Duell, B.L., Bobowski, G., Bristol, J.A. and Evans, D.B., J. Med. Chem., 28 (1985) 1405–1413.
19 Sircar, I., Duell, B.L., Cain, M.H., Burke, S.E. and Bristol, R.A., J. Med. Chem., 29 (1986) 2142–2148.
20 Weishaar, R.E., Caine, M.H. and Bristol, J.A., J. Med. Chem., 28 (1985) 537–545.